Improving Tropical Cyclone Guidance Tools by Accounting for Variations in Size

John A. Knaff[1], Mark DeMaria[1], Scott P. Longmore[2] and Robert T. DeMaria[2]

[1]*NOAA Center for Satellite Applications and Research, Fort Collins, CO*

[2] *CIRA, Colorado State University, Fort Collins, CO*

1. Introduction

Tropical Cyclones (TCs) come in many sizes. The areal extent of largest TC can be 50 times larger than the smallest TC. In terms of radial extent of circulation, differences are generally less than an order magnitude, but are nonetheless important. Representative examples of typical TC size differences among intensities and basins are shown in Figure 1.

Typical TC size metrics like the Radius of Outermost Closed Isobar (ROCI) and operationally significant wind radii (e.g. 34-kt, 50-kt, 64-kt) however are generally of low quality and the methods used estimate these metrics in operations are generally undocumented, and inhomogeneous (between different agencies and over the course of time). Because of these issues with TC size metrics, most TC forecast and diagnostic methods do not explicitly account for TC size variability.

To move forward in this area and begin accounting for TC size variations in our diagnostic and forecast tools, we propose a solution. Our solution is to use an objectively-derived TC size metric that can be derived from routinely available information to unambiguously account for TC size variations. This simple, documented and repeatable method attempts to align the radial tangential winds from the outside inward, which is analogous to scaling by the radius of maximum wind, or from the inside outward, employed by other studies (e.g. Rogers et al. 2012, Zhang and Uhlhorn 2012). By working inward we hope to better separate the structures associated with the outer circulation like principle rainbands, from the structures of the inner core like the eyewall.

We hypothesize that accounting for TC size variations can improve the diagnosis and forecasts of TCs. To test this hypothesis we use the 2013 version of the Statistical Hurricane Intensity Prediction Scheme (SHIPS), the Logistic Growth Model (LGEM) and an experimental version of the Rapid Intensity Index (Kaplan et al. 2010) that uses both infrared (IR) satellite data and lightning density from the World Wide Lightning Location Network (WWLLN, Lay et al. 2004, Rodger et al. 2005). We use the recently developed IR-based TC size estimate, R5, to scale some of the inputs to SHIPS, LGEM and RII. In the simplest terms, R5 is the radius of where the TC wind field is indistinguishable from the background flow in a climatological environment and is a function of radial profile of IR brightness temperatures and latitude, as described in Knaff et al. (2014). Below we will review the derivation of R5, describe and show how R5 can be used to account for TC size variations, followed by a presentation of how this "scaling" of IR- and lightning-based predictors impacts SHIPS, LGEM and RII forecasts.

2. An Objective TC Size Parameter (R5)

An objective IR-based estimate of TC size was created by regressing the sine of the latitude, and the first three normalized principle components (PCs) azimuthally averaged radial profiles of IR brightness temperatures with the dependent variable,

850-hPa average tangential wind at r= 500 km (V500) from the SHIPS large-scale diagnostic files. The EOFs associated with these PCs are shown in Figure 2. The resulting multiple regression equation explains 29% of the variance of observed V500 and has a root mean square error of 2.9 ms-1. The resulting regression equation is provided in equation (1).

$$\mathrm{V500} = 2.488 + 11.478 * \sin|\varphi| - 1.350 * \mathrm{PC1} + 0.912 * \mathrm{PC2} + 0.319 * \mathrm{PC3} \quad (1)$$

In (1), φ is latitude, and PC1, PC2, and PC3 are the normalized principle components. The predicted V500 appears best related to TC size variations and most of the scatter in the relationship results from the variations in the environment (Knaff et al. 2014).

Since TC size implies units of distance or area, the estimated V500 that comes from (1) is scaled using the climatological (1995 to 2011) mean linear relationship between the azimuthally averaged tangential wind at 500 km (V500c) and at 1000 km (V1000c). V1000c is derived from the average (r=0 – 1000 km) vorticity (ζ1000) using this relationship V1000c= rζ1000, where r is the radius. Using the slope of this relationship and an estimate of V500 [i.e., from (1)], the radius where the mean tangential wind at 850 hPa is 5 kt (R5) is found. In Knaff et al (2014) a 5-kt tangential wind at 850 hPa is assumed to be essentially the same as the background flow. The relationship between V500 and R5 is provided in equation (2),

$$\mathrm{R5} = \left(\overline{\mathrm{R5}} + (\mathrm{V500} - \mathrm{V500c}) * \frac{500}{\mathrm{V500c} - \mathrm{V1000c}}\right) \quad (2)$$

where the climatological mean values of R5, V500 and V1000 are $\overline{(R5)}$=952km, V500c=5.05 ms-1, and V1000c =2.23 ms-1, respectively, and V500 is estimated using (1). To make the units more manageable and to allow better comparison with historical work on this subject, R5 is generally presented in units of degrees latitude. Since the predicted V500, and thus R5, is primarily related to vatiations in TC size and not changes in the environment, it is somewhat ideal for categorizing TC size. Complete details of how V500, and R5 were created and how well these metrics are related to TC size can be found in Knaff et al. (2014).

3. Scaling TCs using the R5 TC Size Metric

One of the findings of Knaff et al. (2014) was that R5 generally increases as TCs become more intense and decreases as TC weaken. Using the global climatology of R5 detailed in Knaff et al. (2011) a simple relationship between TC intensity (Vm) and R5, $R5_c$, is derived. The equation for $R5_c$ is provided in (3) and ploted in Figure 3. A simple radial scaling factor F_{R5} is created by dividing the observed R5 by $R5_c$ as shown in (4).

$$R5_c = 7.653 + \left(\frac{Vm}{11.651}\right) - \left(\frac{Vm}{59.067}\right)^2, \quad (3)$$

$$F_{R5} = \frac{R5}{R5_c}, \quad (4)$$

A scaled radius (R_s) is then formed by dividing the physical radius (r) by F_{R5} as shown in (5). For the remainder of this paper we will refer to using the scaled radius in place of the observed radius as “scaling”.

$$R_s = \frac{r}{F_{R5}}, \quad (5)$$

To show examples how scaling affects the spatial distribution of brightness temperatures, the images shown in Figure 1 are scaled and re-displayed in Figure 4. In the case of the more intense storms the scaling (top row) seems to be able to better align the principle rainband features (starting at 150 km or so) and better confine the ring of eyewall convection within ~ 125 km. Figure 5 shows a more dramatic example where the original and scaled IR images of Hurricane Katrina (2005), a very large hurricane, and Hurricane Felix (2007), a very small hurricane, are compared.

Another way to examine how scaling affects the alignment of features is accomplished through compositing

observations, in this case lightning density, by radial distance from the storm center. Figure 6 shows the climatology of lightning density as a function of intensity and both radius and scaled radius for the Atlantic (solid) and East Pacific (dashed). The scaling appears to make the distributions between the generally larger Atlantic TCs and smaller East Pacific TC more similar, noting that in general the East Pacific storms have less lightning (DeMaria et al. 2012). This ability to better align structural features in both the outer region of the storm and near the eyewall of the TC and thus impact forecasts is investigated by examining the current suite of statistical intensity guidance in the next section.

4. Results of Scaling on Statistical Intensity Guidance

To investigate the impact of scaling IR and lightning inputs we modify existing operational and experimental methods to predict intensity change. These include the 2013 versions of SHIPS (DeMaria et al. 2005) and LGEM (DeMaria et al. 2009) and experimental versions of the Rapid Intensification Index (RII, Kaplan et al. 2010). The SHIPS model has 24 predictors, whereas the LGEM has 19 predictors. There are two versions of the experimental RII. The first is based on 1995 – 2012 data and does not include lightning information and has 9 predictors. The model was developed for both the Atlantic and East Pacific. The second version of the RII that is examined makes use of WWLLN lightning data, which has 11 predictors, and is based on 2005-2012 data. Results presented here are based on dependent data and we will concentrate the percent variance explained as a metric of improvement for deterministic SHIPS and LGEM models and on the Brier Skill Score (BSS) and the percent correctly forecasts (PCF) as metrics of improvement for the probabilistic forecasts from RII. The former evaluates the probabilistic errors and the later measure the ability of the discriminant analysis to correctly categorize events.

SHIPS and LGEM use information from the GOES satellites in a very simplified manner. Two predictors are used in both models, namely the number of pixels colder than -20 ^{o}C in an annulus of 50 to 200 km from the storm center (PC20) and the standard deviation of brightness temperatures within 200 km of the center (GSTD). These two predictors were recalculated using scaled radii and tested in the SHIPS and LGEM models. We also tested the use of different brightness temperature thresholds ranging from -10^{o}C to -60^{o}C, collectively referred to as pixel counts. All results suggest that scaling the radii slightly degrades SHIPS forecasts in both the Atlantic and East Pacific. LGEM-based forecasts also showed degradation in both the Atlantic and East Pacific sample. This negative result may be caused by the relatively large number of predictors used for both these models and by the fact that other predictors are not scaled in the same manner. We now shift focus to results from the relatively simple statistical RII model.

The RII model is based on a linear discriminant function that is then fit to the observed frequency of events to provide probabilistic forecasts. Again the GOES IR data are treated in a relatively simple manner (GSTD) and PC30 (-30^{o}C). Here we also test the temperature threshold associated with the pixel count variables from -10 to -60^{o}C. The examination of 1995-2012 RII output shows that scaling the IR-based predictors produce mixed results, with significant improvements being seen in the Atlantic, but slight degradation in terms of BSS resulting in the East Pacific. Figure 7 shows the BSS and PCF as a function of pixel counts for the standard and scaled IR predictors.

The 2005-2012 RII, that makes use of WWLLN lightning density data, was evaluated by running the model without lightning information (9 predictors, two of which are related to IR), with the two lightning predictors, scaling those lightning predictors, scaling the lightning and IR predictors. Lightning predictors are the square root of the lightning density within 200km (LD02) and the square root of the lightning density in an annulus 200-400 km from the storm center

(LD24). Figure 8 (top) shows the average lightning density in 100 km bins stratified by 24-h intensity changes in the Atlantic and East Pacific, where rapid intensification is defined as changes ≥ 30 kt, and rapid weakening is defined as intensity changes ≤ 20 kt. Figure 8 (bottom) shows the same stratifications except that the radial coordinates have been scaled. Notice the shift in the response outward, particularly in the Atlantic. For this reason, and after testing found the relationship best explains rapid intensification, we will use the square root of lightning density in the 0-200 km and 300-500 km regions for testing the scaled lightning response in the RII (i.e. LD02 and LD35).

The results of testing the impact of scaling on the RII with both IR and lightning-based predictors are shown in Figure 9. In general, scaling the predictors resulted in improvements in BSS with the largest improvements found when both IR and lightning predictors are scaled. The largest impact from scaling is observed in the Atlantic basin with scaling increasing BSS by about 1%. Only modest improvements are seen by scaling in the East Pacific and only when colder thresholds are used for the pixel count predictors. One additional result suggest that the RII should probably be making use of a colder pixel count threshold with PC50 producing the best dependent results.

5. Summary and Conclusions

Tropical Cyclones (TCs) come in many sizes (Figure 1), but the size of the TC is rarely accounted for explicitly in the development of diagnostic or forecast techniques. In the past TC metrics like ROCI and wind radii were of low quality, but recent work (Knaff et al. 2014) has provided a simple metric of TC size that is based entirely on IR imagery and storm latitude (R5, equations 1 and 2). This measure of TC size is valid for all intensities. Using intensity information and a global climatology of R5 allows TCs to be radially scaled to explicitly account for size variations (equations 3-5). This simple method aligns the radial distribution of tangential winds from the outside inward, which is analogous to scaling by the radius of maximum wind, or from the inside outward, employed by other studies. We have shown examples of how this metric can be used to scale IR images (Figures 4 and 5).

To test the hypothesis that by accounting for TC size, the diagnosis and forecasts of TCs can be improved, we used the 2013 versions of the SHIPS, the LGEM and an experimental version of the Rapid Intensity Index that uses both IR satellite and lightning density data. We use the IR-based size estimate, R5, to scale the inputs to SHIPS, LGEM and RII. Our preliminary and dependent results suggest that scaling lightning and IR predictors significantly improve the probabilistic forecasts of rapid intensification, but actually degraded the deterministic SHIPS and LGEM models. Our recommendations are to use a colder temperature threshold, -50^{o}C, for future RII applications and to scale IR lightning, and other predictors that vary considerably as a function of TC size/radial extent for future statistical model development and case studies.

Acknowledgements: The authors would like to thank the GOES-R program office and the NOAA Hurricane Forecast Improvement Program for supporting this research. The views, opinions, and findings contained in this report are those of the authors and should not be construed as an official National Oceanic and Atmospheric Administration or U.S. government position, policy, or decision.

References:

DeMaria, M., R.T. DeMaria, J.A. Knaff and D.A. Molenar, 2012: Tropical cyclone lighting and rapid intensity change. *Mon. Wea. Rev*., **140**:6, 1828-1842.

Kaplan, J., M. DeMaria, and JA. Knaff, 2010: A revised tropical cyclone rapid intensification index for the Atlantic and east Pacific basins. *Wea. Forecasting*, **25**, 220-241.

Knaff, J.A., S.P. Longmore, D.A. Molenar, 2014: An Objective Satellite-Based Tropical Cyclone Size Climatology. *J. Climate*, **27**, 455-476.

Lay, E.H., R.H. Holzworth, C.J. Rodger, J. N. Thomas, O. Pinto Jr., and R. L. Dowden, 2004: WWLL global lightning detection system: Regional validation study in Brazil. *Geophys. Res. Lett.*, **31**, L03102, doi:10.1029/2003GL018882.

Rodger, C. J., J. B. Brundell, and R. L. Dowden, 2005: Location accuracy of VLF World Wide Lightning Location (WWLL) network: Post-algorithm upgrade. *Ann. Geophys*., **23**, 277–290.

Rogers, R., S. Lorsolo, P. Reasor, J. Gamache, F. Marks, 2012: Multiscale analysis of tropical cyclone kinematic structure from airborne doppler radar composites. *Mon. Wea. Rev.*, **140**, 77–99.

Zhang, J. A., and E. W. Uhlhorn, 2012: Hurricane sea-surface inflow angle and an observation-based parametric model. *Mon. Wea. Rev*., **140**, 3587-3605.

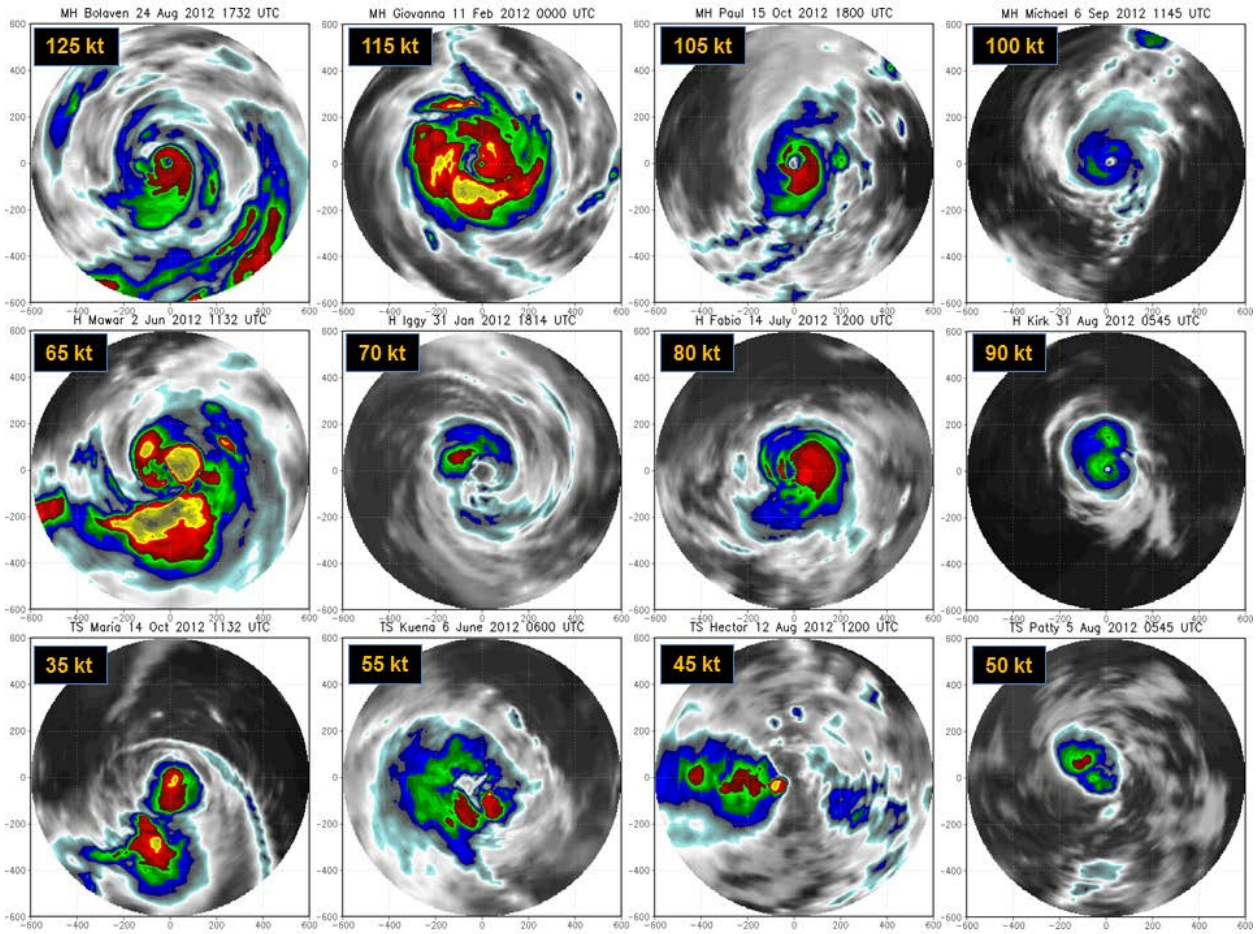

Figure 1. IR images of several TCs that occurred during 2012 that illustrates the variety of shapes and sizes that are observed. Rows show major hurricane, non-major hurricane, and tropical storm intensities, respectively. Columns show storms occurring in the western North Pacific, Southern Hemisphere, East Pacific, and Atlantic basins, respectively.

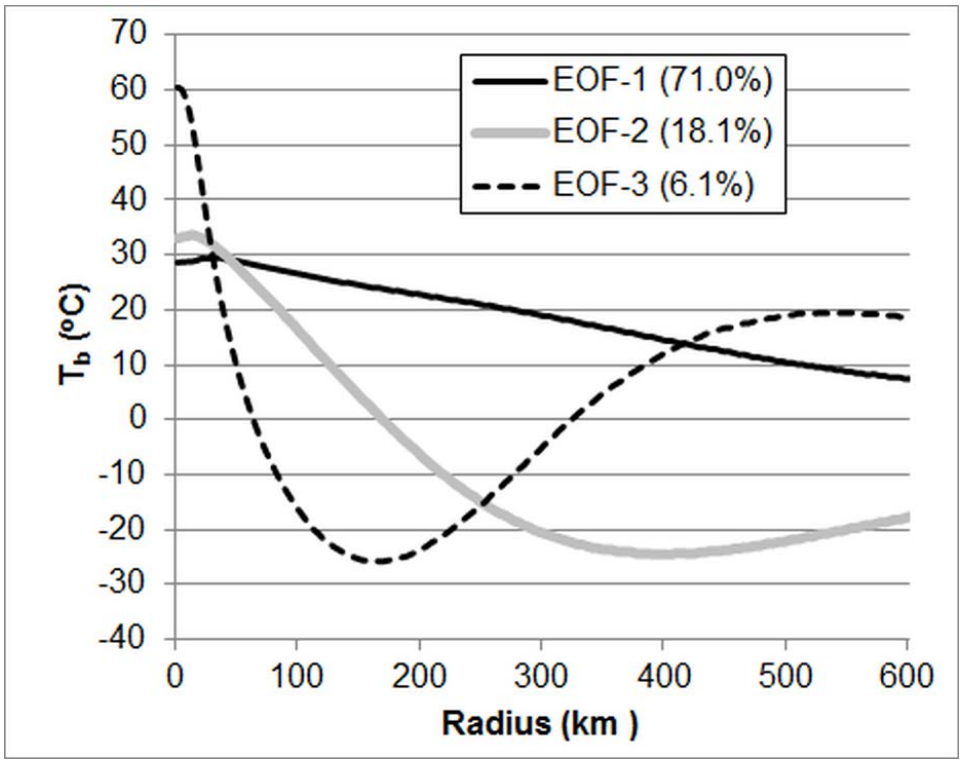

Figure 2. Leading modes of variability or Empirical Orthogonal Functions (EOFs) of the 6-hourly mean azimuthally averaged profiles of IR BT. The percent of the variance explained by each EOF is shown in parentheses.

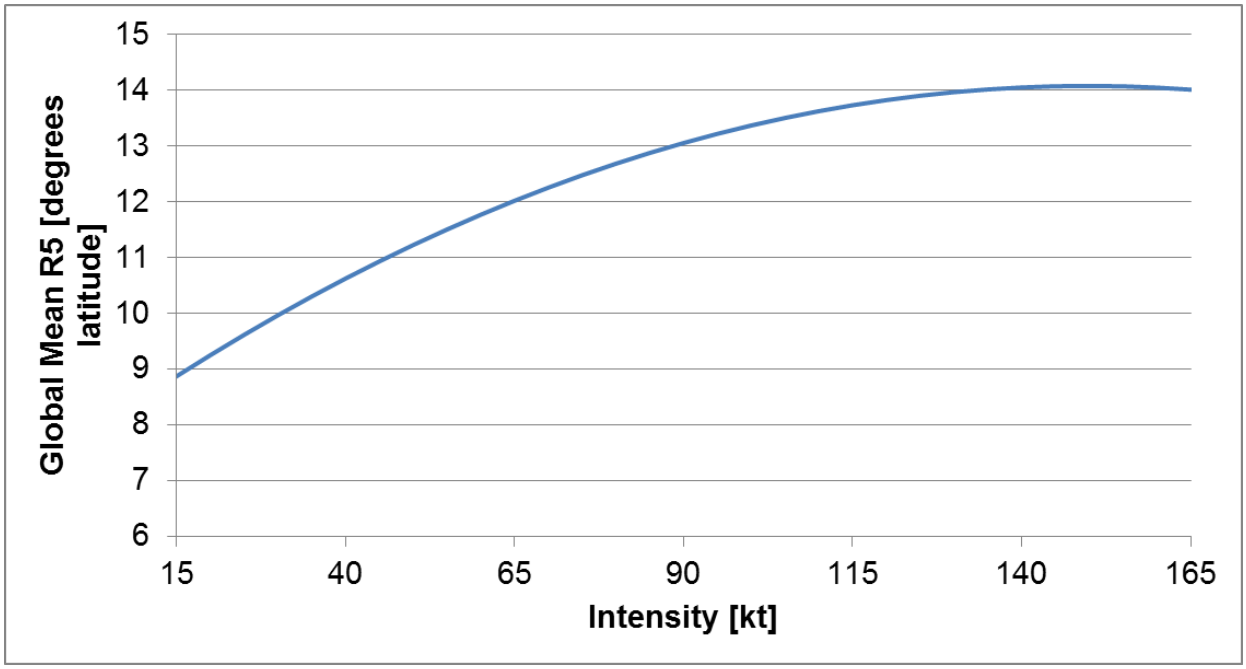

Figure 3. Graph showing the global mean R5 as a function of TC intensity.

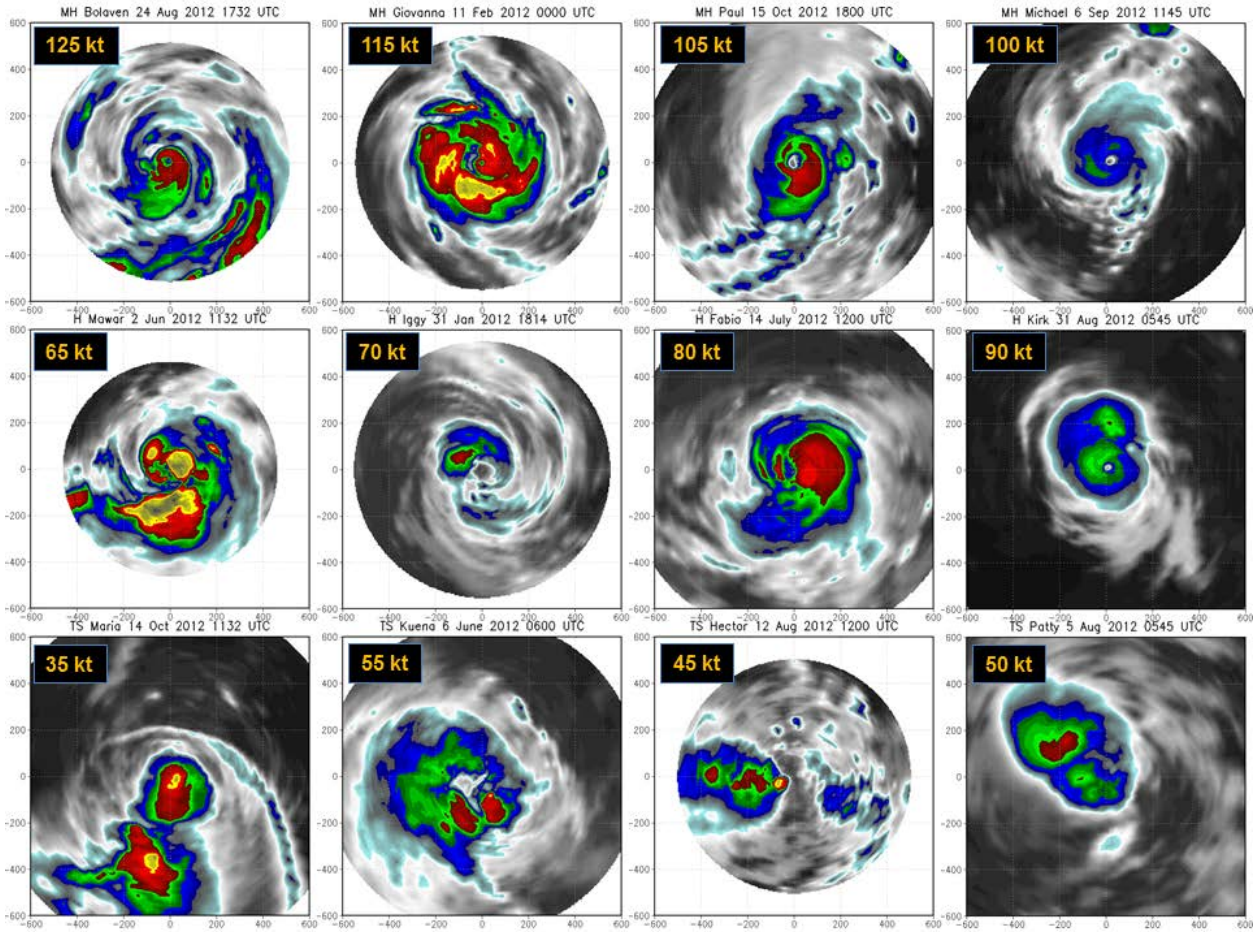

Figure 4. IR images of several TCs that occurred during 2012. These images show the same cases that are shown in Figure 1 except they have been scaled so that there sizes (i.e., radial extent defined by R5) are the same.

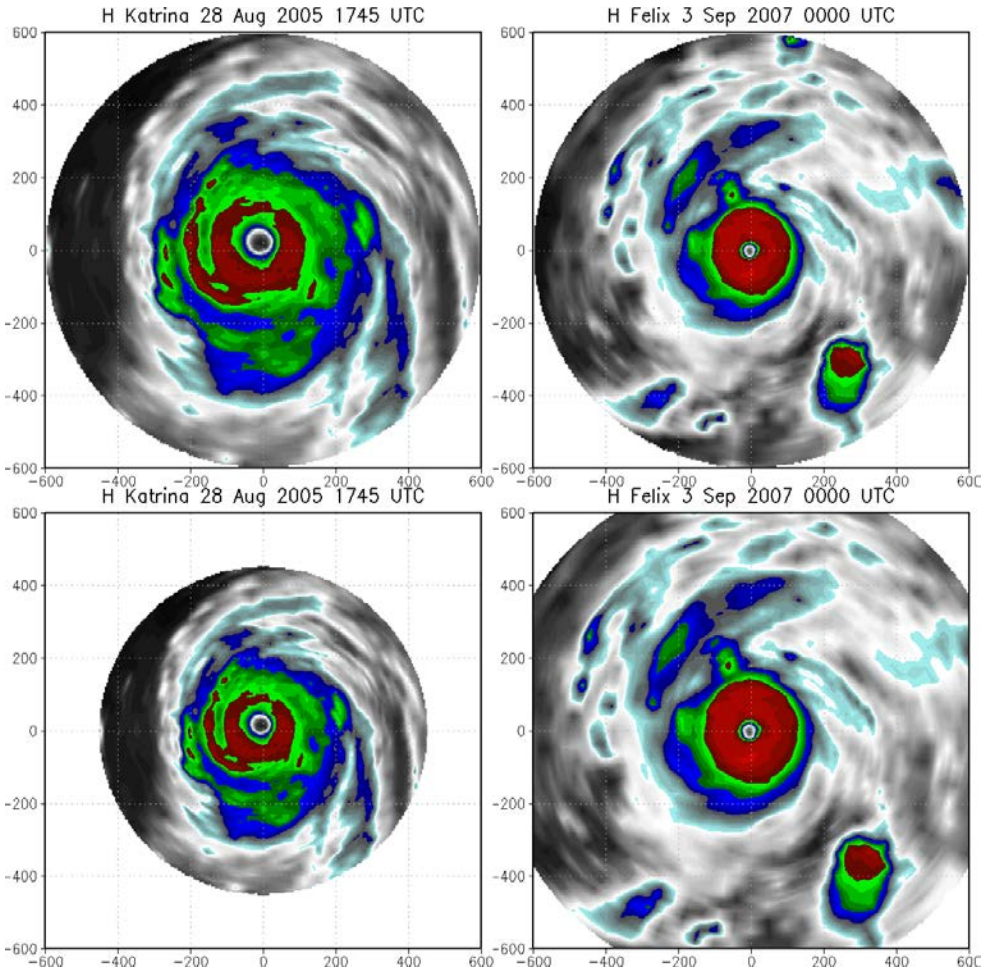

Figure 5. Examples of the effect of scaling IR data are shown. Two major hurricanes are shown. Katrina was a very large TC and Felix was a very small TC. Hurricane Katrina (2005, left) and Hurricane Felix (2007, right). Earth relative coordinates are shown at the top and scaled coordinates at the bottom.

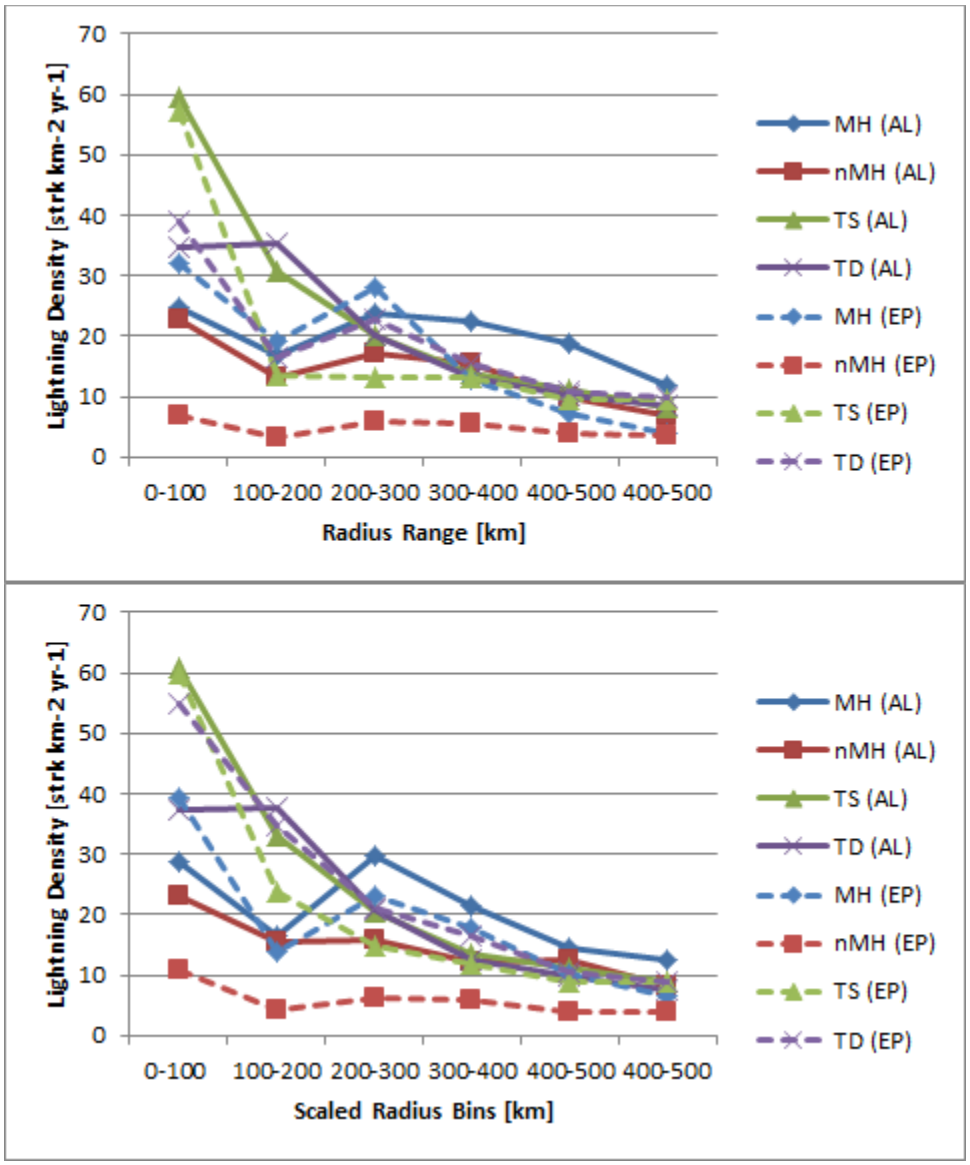

Figure 6. Plot of the storm-relative lightning density climatologies [strikes km^{-2} $year^{-1}$] shown as a function of intensity and radius (top), and intensity and scaled radius (bottom). The plot is based on 2005-2012 and lightning data comes from the World Wide Lightning Location Network.

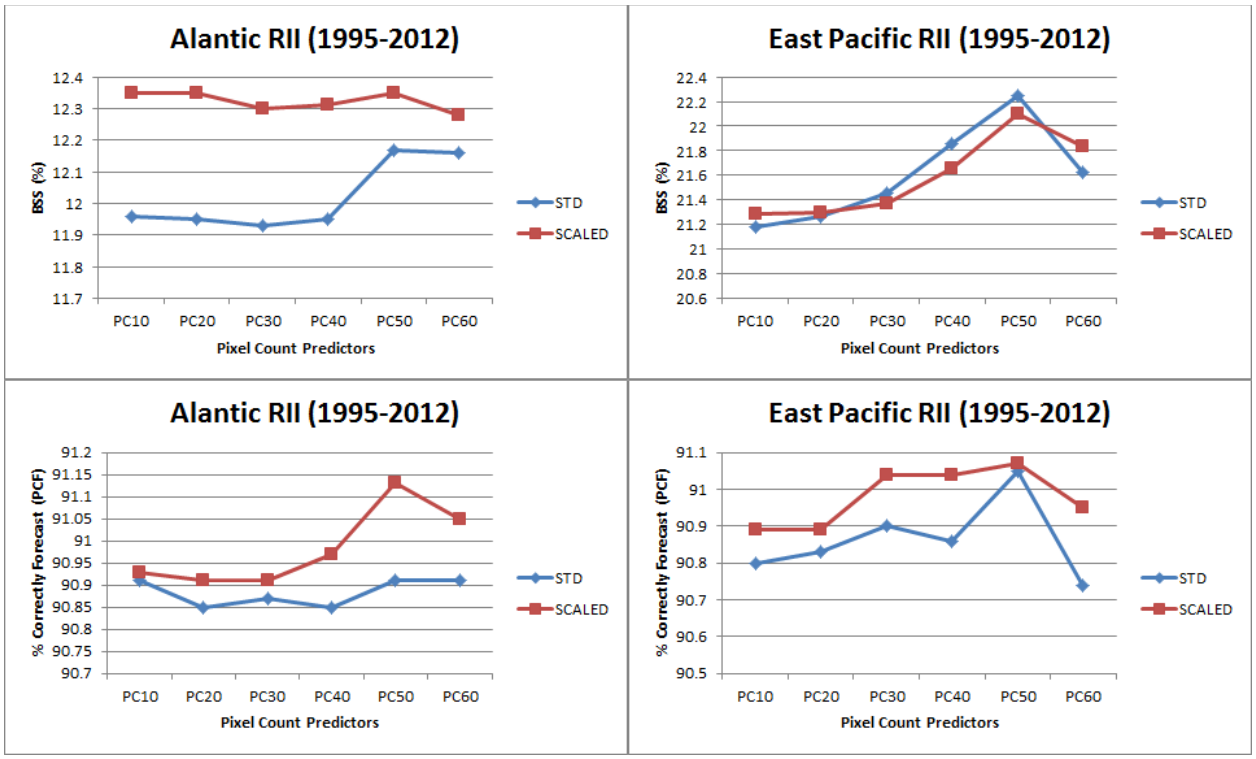

Figure 7. Dependent results based on the experimental version of the RII (1995-2012) run in the Atlantic (left) and East Pacific (right) as a function of pixel count predictors in this model. Results show the impact of scaling the IR predictors as a function of TC size on resulting BSS (top) and PFC (bottom). Blue lines show the control and red lines show the results when IR predictors are scaled.

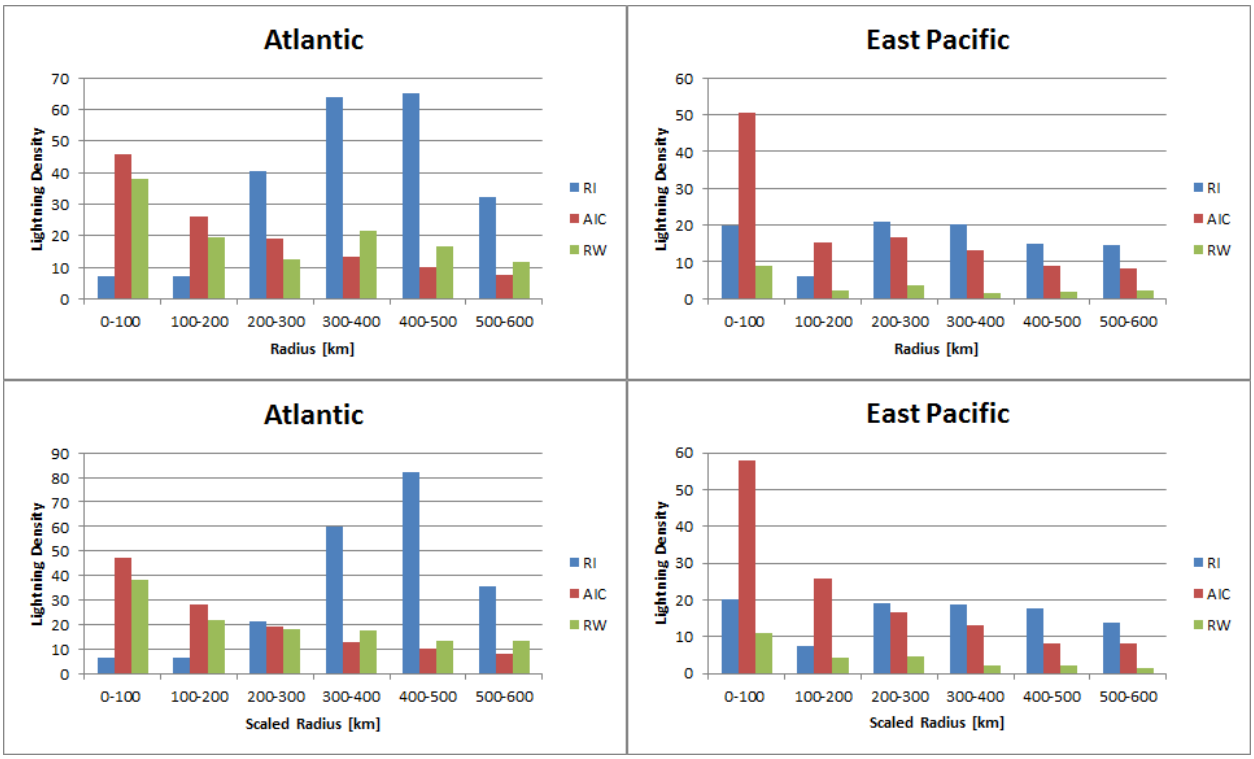

Figure 8. Plots of Atlantic (left) and East Pacific (right) lightning density composites shown as a function of radial distance from the storm center and future intensity changes. Rapid intensification (RI), Average Intensity Change (AIC) and Rapid Weakening (RW) represent case that have 24-h intensity changes (dV) ≥ 30 kt, 30 kt > dV < -20 kt, and dV≤ -20 kt, respectively. Top panels show the observed radial extent and the bottom panels show the composites based on scaled radial distances.

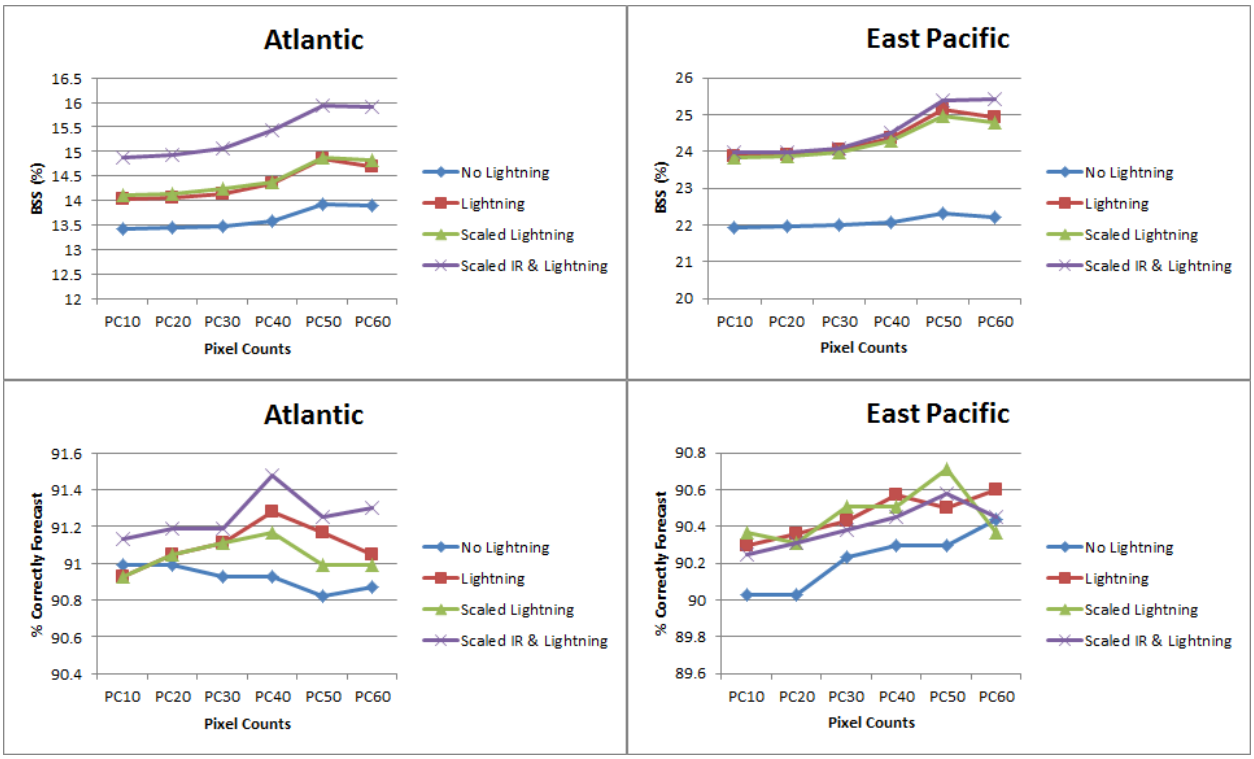

Figure 9. Dependent results from the RII that contains lightning and IR information, 2005-2012, in the Atlantic (left) and East Pacific (right) in terms of variable pixel count predictors. The model developed without lightning information (blue), with lightning information (red), using scaled lightning information (green) and scaled lightning and IR data (purple).